I&EC research
Industrial & Engineering Chemistry Research

pubs.acs.org/IECR
Article

Cost Estimation of the Production of MIL-100(Fe) at Industrial Scale from Two Upscaled Sustainable Synthesis Routes

Published as part of Industrial & Engineering Chemistry Research special issue "MOF2024: From Laboratory to Industry".

Maria Inês Severino, Cátia Freitas, Vanessa Pimenta, Farid Nouar,* Moisés L. Pinto,* and Christian Serre*

Cite This: *Ind. Eng. Chem. Res.* 2025, 64, 2708−2718

Read Online

ACCESS | Metrics & More | Article Recommendations | Supporting Information

ABSTRACT: Understanding the impact of MOF synthesis conditions on the production cost is vital in order to have a competitive product with a view toward industrial applications. Here, considering the benchmark mesoporous iron(III) trimesate MIL-100(Fe) as a prototypical example, we show that the production cost can reach <30 $/kg if a careful selection of the synthetic route is made. Two routes were considered in the analysis, using sulfate and nitrate as iron sources. A new optimized synthesis protocol in a 5 L laboratory pilot-scale reactor based on iron sulfate was developed using optimized sustainable aqueous ambient pressure conditions, leading to larger particles and a higher space-time yield. Based on reliable pilot-scale data and established chemical engineering estimation methods, this leads to a significantly lower production cost of high-quality MIL-100(Fe), achieving a potential competitive product.

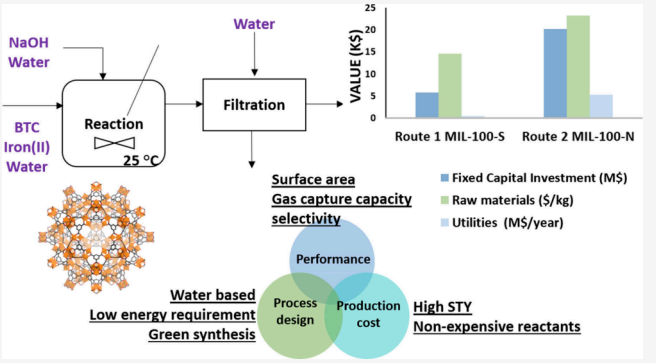

1. INTRODUCTION

Metal−organic frameworks (MOFs) are crystalline porous materials whose discovery was initiated at the end of the 1990s.[1] These solids are attractive for a large range of potential applications such as gas storage/separation, sensing, heterogeneous catalysis, energy devices, and biomedical applications, among others, due to their high porosity and unprecedented chemical and structural versatility.[2] Interest in their real applications has also been increasing recently partly due to the scale-up of a few benchmark MOFs under green, sustainable, and potentially economically viable conditions, as we will briefly highlight in the following paragraphs.[14−18,24−27]

The use of water or other less-toxic solvents is indeed highly preferable,[3−8] and there are currently many examples of water-based MOF synthesis methods in ambient pressure conditions, such as, for instance, those of the MIL family: MIL-100(Fe),[9] MIL-91(Ti, Al),[10,11] MIL-160(Al),[12] and MIL-53(Al)-NO_2 or -NH_2.[13] Furthermore, other industrially relevant aluminum-based MOFs of interest for gas separation or heat reallocation, such as CAU-10(Al), MIL-160(Al), or MOF-303, have also been synthesized using greener protocols at larger scale.[14] The Zr fumarate MOF-801(Zr), of interest for water harvesting, was also obtained with good yield and quality in a 5 L pilot-scale reactor using a modulator.[15] The use of alcohols is also an acceptable alternative, for instance, for the ambient pressure synthesis of MIL-127(Fe) (also known as *soc*-MOF)[16] or the synthesis of the new benchmark MOF for CO_2 capture in flue conditions, CALF-20, produced with a very high space-time yield (STY).[17]

Besides the importance of safety and health impacts, the cost can be reduced by decreasing the energy requirements and/or by requiring less expensive equipment (e.g., built from noncorrosive resistant materials or ambient pressure equipment). Therefore, ambient pressure, low-temperature synthesis associated with the use of nontoxic safe conditions are beneficial as it is overall cheaper and much simpler to scale-up. This requires, however, synthesis optimizations that carefully select not only the solvent and relevant synthesis conditions of pressure and temperature but also the chemical precursors, such as the metal source or the linker, which should be noncorrosive, nontoxic, and abundant. For instance, the use of corrosive counterions should be avoided, and thereby metal carbonates, sulfates and oxides are preferred instead of

Received: July 24, 2024
Revised: December 9, 2024
Accepted: December 11, 2024
Published: January 22, 2025

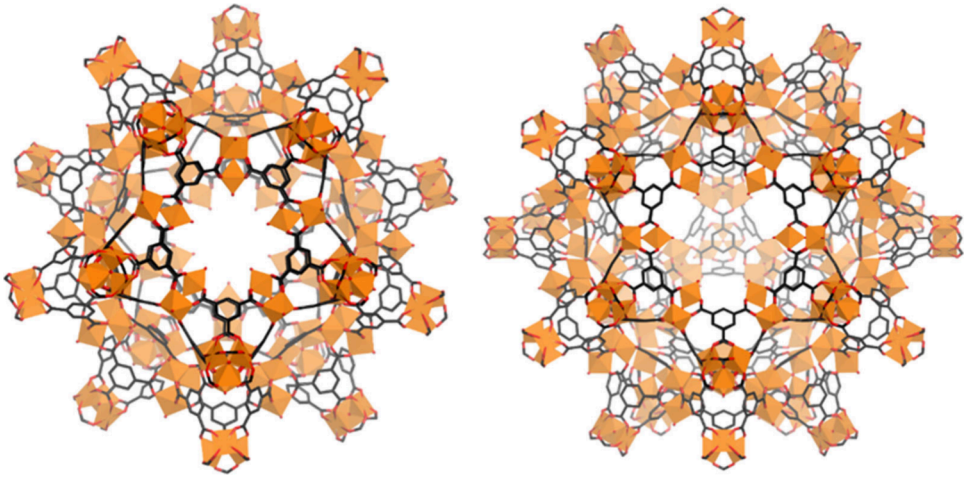

Figure 1. Schematic view of the MIL-100(Fe) structure (CCDC 640536 from ref 30) with the small S cage (left) and large L cage (right) in MIL-100(Fe). Hydrogen atoms are omitted for clarity. FeO_6 octahedra and oxygen and carbon atoms are shown in orange, red, and black, respectively.

chlorides.[7] In addition, the use of sustainable linkers can result in a lower price, minimal environmental impact, and lower toxicity, as well as having a higher water solubility and thus an efficient metal-ion/linker reactivity. This was demonstrated by some of us in the case of the benchmark microporous MIL-160(Al) MOF, of interest for heat reallocation and gas separation, built up from a bioderived ligand.[18]

Despite these promising studies on the improvement of the production greenness, MOFs are still mainly scaled-up either by startups such as Framergy, MOFtechnologies, MOFapps, Promethean Particles (or Nueda), Numat, NovoMOFs, ProfMOF, Immaterial, etc[19] or by large chemical companies such as BASF;[20] however, with the recent exception of CALF-20, still limited amounts are envisioned and are mainly available for research and development purposes or for a particular application in lower scale (<ton).[21] As a result, the costs at higher scale are still either unknown or high when available. Nevertheless, these latter values are not representative of the real production cost which will depend not only on the final purity required, the type of process to be considered, and raw material price for bulk production but also on the scale of production. However, the price can be reduced when the raw materials, e.g., the linker, are used in other large-scale processes, such as, those that are used in the pharmaceutical industries, plastics production, etc. Therefore, depending on the parameters considered, the final production cost is much lower than the cost initially estimated by laboratory scale processes. A few studies have already explored the production cost of MOFs at the multi-ton scale. DeSantis et al. explored different synthesis approaches, liquid-assisted grinding (LAG) and aqueous synthesis, and estimated that the cost of MOFs can be brought down to less than 10 $/kg for a 2.5 ton/year production.[22] UiO-66(Zr)-NH_2 was also recently studied by Luo et al.[23] In this study, solvothermal and ambient pressure aqueous-based syntheses were compared in terms of industrial potential. It was clear that with the same production base, the solvothermal synthesis led to higher costs, with a production cost about 3 times higher than the aqueous-based synthesis, i.e., 44 $/kg vs 15 $/kg. This proves the importance of the choice of the production process and its optimization on the estimated final production cost. However, this estimation was based on a hypothetical process. Before production cost calculation estimations are assessed, it is important to understand the process scalability using laboratory pilot-scale tools. This allows one to bridge the laboratory scale, where only a few milligrams or grams are produced, and the industrial scale, where tonnage of the material is produced, confirming the scalability and optimizing further the process at the 100 g or kilogram level. This has been done, but not extensively, for several benchmark MOFs, for instance, ZIF-8 producing 6 kg per day in a continuous flow,[24] UiO-66(Zr) and its functionalized derivatives UiO-66(Zr)-NH_2 and its −COOH form in a solvothermal system giving 647 g in 8 L,[25] or CAU-10(Al) with 6 kg produced in 10 L in a 10 h reflux synthesis.[26,27]

More recently, an important breakthrough in MOFs was reported with the announcement of the tonnage production of the microporous Zn triazolate-oxalate CALF-20. This MOF, initially reported by Shimizu et al., will be produced by BASF in partnership with Svante at multihundred ton scale, and the production cost is expected to reach <30 $/kg for the capture of CO_2 in cement fabrication.[28,29] With this recent announcement, it was seen that coupling the high performance potential with the optimization of the production process is essential to achieving scalable production. Furthermore, estimation of the production cost of some of these materials can help potentiate the consideration of MOF production in industrial applications.

A comprehensive cost assessment methodology has been recently proposed for the prototypical MOF, MIL-160(Al), based on its production in a pilot-scale reactor, whereas the production cost at industrial scale was estimated to be 55 $ and 29.5 $ per kg for 100 tons and 1 kton, respectively, and reaching costs below 10 $/kg, at a condition that its constitutive bioderived linker, 2,5-furandicarboxylic acid, is to be utilized at very large scale for the production of bioplastics.[18]

Here, we report the production cost estimation at the kton scale for the benchmark MIL-100(Fe), based on a newly developed synthesis protocol, optimized to reach high STY while maintaining compounds with high surface areas and other adsorption properties.

MIL-100(Fe) or $[Fe_3O(OH)(C_6H_3(CO_2)_3)_2 \cdot (H_2O)_2] \cdot nH_2O$ is an iron(III) tricarboxylate MOF built up from trimers of iron octahedra sharing a common vertex μ_3-O.[30,31] These trimers are then linked by the benzene-1,3,5-tricarboxylate

https://doi.org/10.1021/acs.iecr.4c02618
Ind. Eng. Chem. Res. 2025, 64, 2708−2718

Table 1. Ambient Pressure Synthesis Reported in the Literature for MIL-100(Fe), Precursors and Conditions Used, and Characteristics of the Material Obtained

Iron source	Solvent	Modulator	T (°C)	Time (hours)	S_{BET} ($m^2 \cdot g^{-1}$)	V_{total} ($cm^3 \cdot g^{-1}$)	STY ($kg \cdot m^{-3} \cdot day^{-1}$)	ref.
Fe^0	Water (DMF)	Benzoquinone/HNO_3	RT[a]	12	2482[b]	1.0024	–	47
$Fe(NO_3)_3$	DMSO	HNO_3	130	24	1791	0.82	43[c]	48
$Fe(NO_3)_3$	Water (Ethanol)	–	90	18	1212	–		49
$Fe(NO_3)_3$	Water	–	60	48	1800		1.6	43
$FeCl_3$	Glycol/DMF	–	80	2	2037	1.276	–	50
$FeCl_2$	Water (Ethanol)		RT	24				55
$FeCl_2$	Water (Ethanol)	NaOH	RT	4	2097	0.81	99[c]	58
$FeSO_4/FeCl_3$	Water	NaOH	RT	24	1180/650	1.68	17[c]	56
$FeSO_4$	Water	NaOH	RT	24	1893	1.024	21[c]	57
$FeSO_4$	Water (ethanol)	NaOH	RT	15	1542	–	14[c]	61
					2012	–	3[c]	

[a]RT, room-temperature synthesis. [b]Purified with NH_4F [c]Calculated with 100% yield and/or considering reaction volume

moieties that lead to the formation of hybrid supertetrahedra which delimit mesoporous cages of free apertures of 25 and 29 Å, accessible through microporous windows of 5.5 and 8.6 Å (Figure 1). MIL-100 exhibits a very good chemical and thermal stability, a high porosity, and the presence of accessible active sites, allowing the coordination of different species. It also possesses a biodegradable character associated with a low *in vivo* toxicity.[32,33] These unique characteristics make MIL-100(Fe) appealing for a wide range of applications such as biomedicine,[34,35] gas storage/separation,[36−38] sensing,[39] catalysis,[40−42] and heat reallocation.[43,44] More recently, we have shown that this MOF, through its open metal sites, can lead to exceptional properties such as either the capture of traces of acidic volatile organic compounds in humid environments[45,46] or, once reduced, for the unprecedented environmental degradation of NOx at room temperature;[51] in the present work we confirm that the scaled-up production yields materials with similar exceptional properties.

A method is developed here to produce high-quality MIL-100(Fe) along with a high STY. There is indeed a clear need to develop new green and cost-effective synthesis protocols for this benchmark MOF. In this view, we further studied the impact of the metal precursors on the synthesis and the overall cost of the material. Early methods of MIL-100(Fe) preparation were based on hydrothermal conditions. The small-scale protocol reported initially by Horcajada et al.[30] involved iron metal and hydrogen fluoride (HF). A fluoride-free hydrothermal synthesis was later reported by Seo et al.[9] Despite the high space-time yield (STY), >250 $kg \cdot m^{-3} \cdot day^{-1}$ (STY, kg of MOF per m^3 of reactor per day), the use of pressurized hydro/solvo-thermal conditions is not ideal for scale-up production due to safety concerns and high (equipment and energy) costs.[7]

A series of ambient pressure synthesis routes have since then been reported for the preparation of MIL-100(Fe), as shown in Table 1. Some of us have reported very recently a low-temperature green protocol to produce nanoparticles MIL-100(Fe) with a controlled polydispersity suitable for biomedical applications.[52,53] High quality, well faceted 50−60 nm nanoparticles with a low polydispersibilty index (around 0.2−0.25) with high specific surface area (more than 1750 m^2/g) were obtained.[54] However, the diluted synthesis conditions, associated with a low STY, could lead to higher production costs, although this might not be a major issue for biomedical applications. Guesh et al. proposed in parallel another ambient temperature route with a higher STY (around 30 $kg \cdot m^{-3} \cdot day^{-1}$),[55] with however the use of corrosive chlorides, which would imply a higher production cost due to strict requirements in the equipment construction material as well as increasing safety requirements.[7] On the other hand, the use of sulfate counteranion, which is less corrosive, is highly beneficial for the large-scale production of MOFs and has been demonstrated previously for other high valence MOFs such as UiO-66 type materials or CAU-10(Al).[25,27] In the case of MIL-100(Fe), this could be strongly beneficial and has also been reported.[55,56] Nevertheless, although greener synthesis conditions are used, the corresponding STY did not exceed 21 $kg \cdot m^{-3} \cdot day^{-1}$, reinforcing the need to further optimize the synthesis conditions prior to production cost estimation on the industrial scale. The production optimization study in the present work was therefore guided by the need to produce a material with optimum specific surface area (>1700 m^2/g) and to increase the space-time yield while maintaining sustainable conditions, including low energy and materials requirements, suitable for a higher economic viability.[18,23] To assess the quality of upscaled MIL-100(Fe), its performance was finally compared to the values reported previously in the literature for the capture of traces of the polar volatile organic compound (VOC) acetic acid under environmental conditions. The two synthesis routes, relying on either iron(III) nitrate or iron(II) sulfate as iron sources,[52,53] were considered, and different parameters were optimized in terms of STY and quality (porosity, particle size, etc.), such as temperature, concentration, etc.

This led to monodisperse small size nanoparticles with a low STY for the nitrate route, while the sulfate protocol led to much larger particles with a higher STY. The production cost was, therefore, estimated for each metal source based on the optimized conditions, and the different elements of the production cost were finally compared and discussed, providing a comprehensive view of the effect of the synthesis route on MOF production cost.

2. MATERIAL AND METHODS

2.1. Materials. All chemicals were purchased from commercial suppliers and used as received without further purifications: 1,3,5-benzene tricarboxylic acid, 98%, Alfa Aesar; iron(II) sulfate heptahydrate, 98%, Sigma-Aldrich, and sodium hydroxide pellets, 98%, Alfa Aesar; iron(III) nitrate nonahydrate, >99%, Alfa Aesar.

2.2. Synthesis. *2.2.1. Nitrate-Based Synthesis (MIL-100-N). Laboratory Pilot-Scale Synthesis.* MIL-100(Fe)-N was

https://doi.org/10.1021/acs.iecr.4c02618
Ind. Eng. Chem. Res. 2025, 64, 2708−2718

Table 2. Different Reaction Conditions Tested in the Optimization and Respective STY of the Reaction Step for a 12 h Synthesis in a 100 mL Flask

	Ligand (g)	Iron(II) sulfate heptahydrate (g)	Sodium hydroxide (g)	Yield (%)	STY ($kg{\cdot}m^{-3}{\cdot}day^{-1}$)
MIL-100(Fe)-S1	0.85	1.67	0.49	87%	15
MIL-100(Fe)-S2	2.55	5.01	1.46	67%	68
MIL-100(Fe)-S3	4.25	8.34	2.42	64%	95

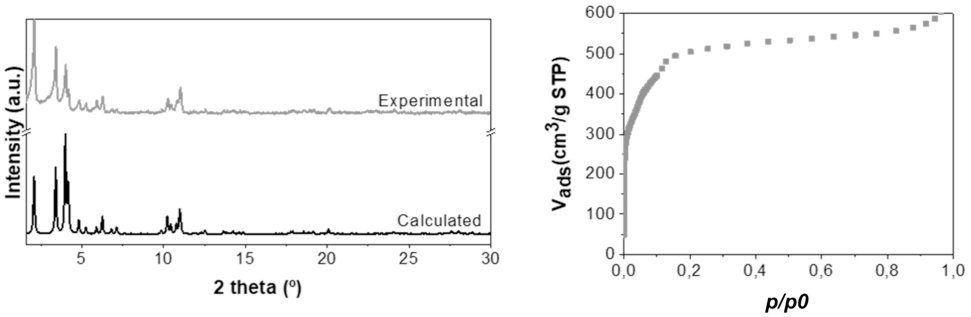

Figure 2. PXRD pattern of MIL-100(Fe)-N synthesized in a 5 L pilot-scale reactor with iron(III) nitrate nonahydrate, in 2θ range 1.6−30°, compared with the calculated pattern from the literature (Cu Kα radiation, λ = 1.5418 Å)[30] (left). Nitrogen adsorption, at T = −196 °C, of MIL-100(Fe)-N in a 5 L pilot-scale reactor with iron(III) nitrate nonahydrate (right) (P_0 = 1 atm.).

obtained via ambient pressure synthesis adapted from the conditions reported in the literature.[53] In a 5 L reactor, 22.4 g of 1,3,5-benzene tricarboxylic acid (BTC) and 64 g of iron(III) nitrate nonahydrate were added initially to 4 L of deionized water. The mixture was heated to 60 °C and mechanically stirred. After 3 h, the same amount of precursors was added. After a 62 h reaction, the brown mixture was filtered to obtain a brown solid, which was washed at room temperature several times with environmentally friendly solvents such as water (2 L) and absolute ethanol (1 L) to remove unreacted precursors including 1,3,5-benzene tricarboxylic acid. The powder was then dried at room temperature (yield = 93% and STY of the reaction ≈ 10 $kg{\cdot}m^{-3}{\cdot}day^{-1}$).

2.2.2. Sulfate-Based Synthesis (MIL-100-S). The sulfate route was optimized in two stages. First the chemical parameters and washing steps were tuned to optimize the synthesis at the scale of a few grams in terms of crystallinity, purity, and STY. Then the scale-up at the laboratory pilot scale using a 5 L reactor was realized.

Small-Scale Optimization. Different concentrations were tested, with constant molar ratio (Table 2), and several samples were taken at various synthesis times until 12 h to monitor the synthesis (crystallinity, purity, yield). The resulting MOF powders were washed directly in the filter with water to remove the unreacted precursors before being dried in a vacuum oven for 15 h at 150 °C.

The optimized protocol, i.e., the conditions to obtain a material with the highest STY while keeping a high purity and surface area, is as follows: 8.34 g of iron(II) sulfate heptahydrate and 4.25 g of 1,3,5-benzene tricarboxylic acid (BTC) were added to 40 mL of deionized water and stirred vigorously for 5 min at room temperature. 2.42 g of NaOH was dissolved in 40 mL of deionized water and added dropwise to the mixture of iron salt and BTC. The solution of 1.5:1:3 = Metal: Ligand: NaOH molar ratio was vigorously stirred at room temperature for a total of 12 h.

The evolution of the synthesis was also followed by changes in color. After the slow addition of the NaOH solution to the iron salt and BTC solution, an initial green precipitate is formed. The solution color slowly turns to yellowish-green and then to orangish-brown, attributed to the slow oxidation of Fe(II) into Fe(III) required for the formation of iron(III) oxo-trimers of the MIL-100(Fe) structure. When the quantity of NaOH was further increased the green solid turned black after just a few minutes, which has been previously attributed to the formation of Fe_3O_4 nanorods.[58]

Laboratory Pilot-Scale Synthesis. Using the above-mentioned optimized conditions, the process was scaled-up by performing the reaction in a 5 L pilot-scale glass reactor using mechanical stirring. 315.5 g of iron(II) sulfate heptahydrate and 162.4 g of 1,3,5-benzene tricarboxylic acid were added to 1.5 L of deionized water and stirred vigorously for 5 min at room temperature. 92.8 g of NaOH solution was dissolved in 1.5 L of deionized water and added dropwise (15 min dropwise addition) to the mixture of iron salt and BTC. The brown solution was kept under vigorous stirring at room temperature for 10−24 h. The resulting MOF was washed directly in the filter with 6 L of water to remove the side products and unreacted linker before being dried in a vacuum oven for 15 h at 150 °C (yield = 93% and STY of the reaction (washing solvent not included) ≈ 120 $kg{\cdot}m^{-3}{\cdot}day^{-1}$).

2.3. Materials Characterization. Routine powder X-ray diffraction (PXRD) data were recorded using a high-throughput Bruker D8 Advance diffractometer working in transmission mode and equipped with a focusing Göbel mirror producing Cu Kα radiation (λ = 1.5418 Å) and a LynxEye detector. Transmission infrared spectra were acquired by a Nicolet iS5 FTIR ThermoFisher spectrometer in the range from 4000 to 400 cm^{-1}. Thermogravimetric analysis was performed with a Mettler Toledo TGA/DSC 2, STAR System apparatus under oxygen flow at a constant heating rate of 5 °C min^{-1}. A scanning electron microscope (SEM, FEI Magellan) equipped with an energy dispersive X-ray spectrometer (EDX) was used to acquire images as well as to perform elemental analyses on the synthesized products. The particle size distribution was estimated by using "ImageJ" software for SEM image processing and analysis. The evaluation of the BET surface area was carried out from nitrogen sorption isotherms measured at −196 °C in a volumetric automatic apparatus

https://doi.org/10.1021/acs.iecr.4c02618
Ind. Eng. Chem. Res. 2025, 64, 2708−2718

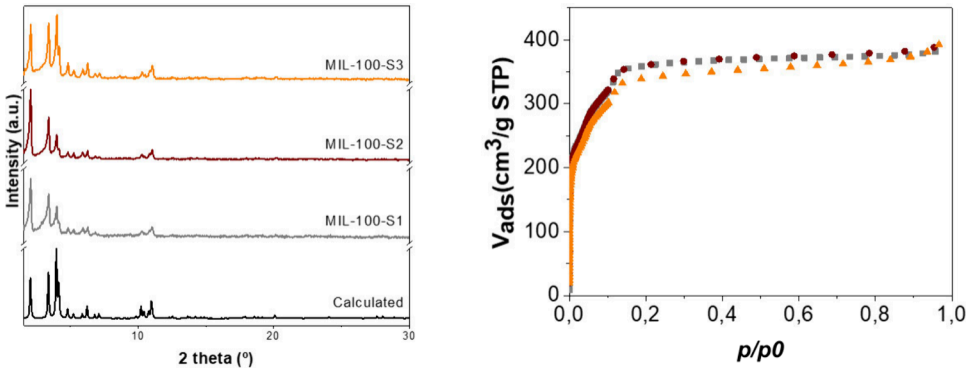

Figure 3. PXRD patterns of MIL-100(Fe) synthesized in 100 mL round-bottom flasks at different concentrations MIL-100-S3 (orange), MIL-100-S2 (brown), and MIL-100-S1 (gray) in 2θ range 1.6−30° compared with calculated pattern[30] (black) (Cu Kα radiation, λ = 1.5418 Å) (left). Nitrogen adsorption isotherms, at T = −196 °C, of all the MIL-100(Fe) samples obtained with different concentrations after 12 h synthesis (orange triangles) MIL-100-S3, (brown circles) MIL-100-S2, and (gray squares) MIL-100-S1 (right) (P_0 = 1 atm.).

(Micromeritics Tristar), after activation under vacuum at 150 °C for 15 h.

3. RESULTS AND DISCUSSION

3.1. Nitrate-Based Synthesis (MIL-100-N). The increase in concentration of the nitrate-based synthesis, adapted from a previously reported protocol developed by some of us, was successfully achieved by the addition of the same amount of precursors after 3 h of reaction.[53] With this improvement, the STY increased by a factor of 6, i.e., from 1.6 kg·m^{-3}·day^{-1} to 10 kg·m^{-3}·day^{-1}, while keeping a monodisperse particle size distribution and an average particle size much lower than 100 nm (Figure S1). The purity of the phase was confirmed by PXRD in comparison with the calculated pattern (Figure 2, left). The absence of unreacted ligand was also verified by FTIR (Figure S2). In addition, the product of the optimized synthesis showed similar adsorption of nitrogen at −196 °C (Figure 2, right) compared to the one reported previously with a BET surface area estimated around 2000 m^2 g^{-1}, which is, to the best of our knowledge, the highest surface area obtained for nanoparticles of MIL-100(Fe) (less than 100 nm). The thermal analysis results under oxygen are well within the expected range losses (Figure S3). This successful laboratory pilot-scale synthesis enabled the production cost estimation for this protocol.

3.2. Sulfate-Based Synthesis (MIL-100-S). *3.2.1. Small-Scale Optimization (MIL-100-S1, S2, and S3).* This optimization work aimed at improving the STY as well as the specific surface area of a previously reported green synthesis protocol using iron(II) sulfate heptahydrate as a metal precursor.[56] We produced samples denoted as MIL-100(Fe)-SX (X = 1, 2, 3) with different concentrations, as summarized in Table 2. Besides the increase in concentration, the main differences of the optimized synthesis with regard to the one reported in the literature was the dropwise addition of the sodium hydroxide solution in the metal/ligand aqueous mixture and the shorter synthesis time. The purpose here was to increase the concentration of the reactants to maximize the STY while maintaining high quality for the final compound. However, to avoid a sharp increase of the pH, a dropwise addition was necessary to slowly deprotonate the ligand while allowing a more controlled metal−ligand reaction and therefore a successful crystallization of MIL-100(Fe). At these high metal/ligand/base precursors concentration levels, i.e., about 5 times higher than previously reported protocols,[56] if a solution of base is added in one step, the pH will sharply rise, promoting the formation of iron oxide particles and/or unwanted coordination polymers. In contrast, our dropwise method allows for a controlled high-concentration synthesis while maintaining high-quality compounds. The product was formed after 4 h for the variable concentrations studied, denoted MIL-100(Fe)-S1, MIL-100(Fe)-S2, and MIL-100(Fe)-S3 (Figure 3, left). The FTIR spectroscopy confirmed the absence of unreacted linkers in all the samples characterized after 4 h (Figure S4). Furthermore, no crystalline impurities were observed in the diffraction pattern, as shown in Figures S5 and S6. It is of note that the use of sulfate metal precursors has been previously reported as being problematic for zirconium-MOF synthesis. The issue was attributed to the strong interaction between the sulfate anions and the framework. For instance, in the case of UiO-66(Zr)-F$_4$, the removal of sulfates required a costly treatment in water at elevated temperature which was only partially achieved (decreasing the SO_4^{2-} ions/Zr_6-cluster ration from 3.6 to 3 after wash).[59] In this work, the sulfate contamination for MIL-100(Fe) was monitored through EDX analyses, as shown in Table S2. An initial sulfur content of 22 atomic% was observed for the unwashed sample that corresponds to a S/Fe molar ratio of around 0.2. However, opposite to the UiO-66(Zr)-F$_4$ case, a simple washing step with water at room temperature directly through the filter eliminated the contamination. The same was observed for the sodium, suggesting that the initial sulfate contamination was only related to unreacted precursors. Such a difference is likely due to the lower Lewis-acidic character of iron(III) compared to zirconium(IV) and thus the lower interaction between the iron sites and sulfates. BET surface areas calculated from the nitrogen isotherms of the samples obtained at different concentrations and 12 h synthesis time (Figure 3, right) reach values above 1600 m^2 g^{-1} for all three samples.[60] Nevertheless, these values are still lower than the ones obtained with the nitrate-based synthesis. Such differences of surface area are tentatively assigned to the differences in quality of the samples, previously attributed by Zhuang et al.[56] to agglomerated forms of nanocrystals and unreacted species (in trace amounts not visible in the FTIR spectra but sufficient to affect adsorption) trapped in the pores. These effects were evidenced by comparing the SEM images at different reaction times. With a synthesis time of 4 h, microrods were observed, probably associated with the formation of a nonporous iron(II) trimesate. In this case, the

https://doi.org/10.1021/acs.iecr.4c02618
Ind. Eng. Chem. Res. 2025, 64, 2708−2718

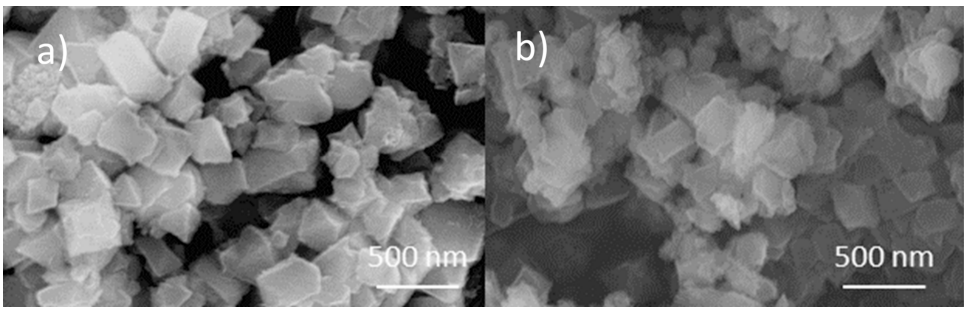

Figure 4. Comparison of SEM picture of the MOF obtained with synthesis with different concentrations, (a) MIL-100(Fe)-S1 and (b) MIL-100(Fe)-S3, for 12 h synthesis.

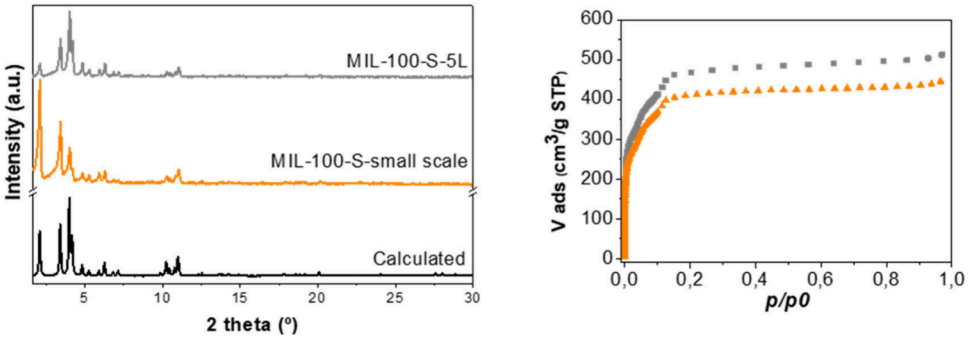

Figure 5. PXRD patterns for MIL-100(Fe) synthesized the 5 L pilot-scale reactor, reactor MIL-100-S-5L (gray) compared with the small scale PXRD (orange), in 2θ range from 1.6 to 30°, and with the calculated pattern (black) (Cu Kα radiation, λ = 1.5418 Å) (left), nitrogen adsorption, at −196 °C (P0 = 1 atm.), isotherms of MIL-100(Fe) synthesized in the 5 L pilot-scale reactor: MIL-100-S-5L (right) and MIL-100-S-small scale (orange) (right).

incomplete reaction led to a lower surface area of 1180 m^2 g^{-1}. Nevertheless, it was shown that the microrods completely disappeared at 24 h of reaction according to SEM. Therefore, to confirm that this was the reason behind the decrease in surface area in our work, MIL-100(Fe)-S3 was left for a 24 h synthesis. The increase in reaction time led to an increase of surface area, reaching around 1850 m^2 g^{-1} (Figure S7).[57,61] It is of note that, in the recent work by Steenhaut et al.,[61] this value of surface area was obtained after only 15 h, and thus, 15 h instead of 24 h could be sufficient to obtain high-quality MIL-100(Fe). Furthermore, one important characteristic of the sulfate route is the formation of larger particles without requiring the use of harsher energy, demanding hydrothermal conditions. The particles obtained, although polydisperse whatever the concentration, exhibit a very similar average size value, above 340 nm for the higher concentration (MIL-100(Fe)-S3) and 320 nm for the lower concentration MIL-100(Fe)-S1 (Figure 4). The microrods described in the literature were not observed in our case for the 12 h synthesis. The obtained particle sizes are higher than the ones reported via other atmospheric pressure synthesis protocols.[52,58] This is advantageous for most industrial uses in general since smaller particles are harder to handle during the production process and final applications and can lead to safety issues. Nevertheless, smaller particles could be an advantage for bioapplications, sensing, or catalysis, and as such, the nitrate optimization synthesis protocol was also explored, although it exhibited a lower STY.

3.2.2. Laboratory Pilot-Scale Synthesis (MIL-100-S-5L). Given the promising results from the optimized small-scale sulfate synthesis, a first upscaling was performed in a larger-scale 5 L pilot reactor. The resulting MOF (MIL-100(Fe)-S-5L) showed good crystallinity, with its PXRD pattern matching the calculated one and that of the small-scale sample (Figure 5, left). To assess the quality of the MIL-100(Fe)-S-5L sample, nitrogen porosimetry analysis was carried out (Figure 5, right), showing an improvement in comparison with the small-scale, with around 1900 m^2 g^{-1} being obtained after only 10 h of reaction. Furthermore, this value is similar to that of MIL-100-N (Figure 2, right) and is consistent with literature values for non-HF routes.[47] This improvement is probably due to more efficient mixing attained with mechanical stirring in the pilot-scale reactor. Therefore, vigorous stirring was considered essential in this reaction, allowing the improvement of the ligand solubility and avoiding abrupt pH increase upon adding the sodium hydroxide solution. To assess the quality of the optimized sulfate-based MIL-100(Fe) material, and in line with our previous findings,[45] the performance of this MOF was assessed for the capture of acetic acid (AA) for the preservation of cultural heritage artifacts, where it is required to capture traces of AA in the presence of a controlled humidity (40−60%RH) at room temperature. It was shown indeed that the mechanism in play was a direct coordination of AA onto the iron open metal sites, replacing water even under high humidity conditions. Thus, such AA capture tests are believed to be excellent candidates for a validation of the accessibility of the metal sites in MIL-100(Fe), while the total nitrogen uptake deduced from nitrogen porosimetry is another complementary tool to compare the total pore volume. The adsorption capacity of traces of AA in controlled humidity environment (40%RH) was used to compare the performance of MIL-100(Fe)-S-5L with our previous adsorption results.[45]

The adsorption of AA under humid conditions for this material was similar to that of MIL-100(Fe)-N and led to a

https://doi.org/10.1021/acs.iecr.4c02618
Ind. Eng. Chem. Res. 2025, 64, 2708−2718

decrease of the AA concentration after 2 h, reaching values lower than 30 $\mu g \cdot dm^{-3}$, in agreement with what was reported before for MIL-100(Fe) (Figure S10). Thus, as the pore volumes deduced from nitrogen porosimetry are comparable, the high quality of the MIL-100(Fe) scaled up using our new sulfate protocol was validated and was the starting point for the techno-economic production cost estimation.

3.3. Production Cost Estimation. The demonstration of the scalability of the nitrate or sulfate synthesis route has been established and paves the way for a preliminary process design. This was done considering all the specifications, the mass balance, and the process design, including the most common pieces of equipment (Figure S11) (the base equipment of the process). Each piece of equipment was sized based on the mass balance of the process and on known heuristics. The output and input compositions of the main streams are shown in Table 3. The price of each piece of equipment or group of equipment based on the mass balance for a 1 kton/year production facility is shown in Table S5. However, the fixed capital investment (FCI) represents not only the capital needed for the installed process equipment but also all the process auxiliaries (e.g., foundations, buildings, structures, piping). Two methods were used to estimate the total FCI: cost factors estimate method and Lang's method, which are further detailed in Table S5. In the cost factor estimation method, typical percentages of the base equipment cost are used to estimate the several portions of the direct and indirect costs (i.e., the FCI), while in the Lang's method a factor over the base equipment investment is used to estimate the FCI considering a process with fluids and solids.[62] The higher FCI estimated was obtained with the cost factor method; this value was thus chosen for the production cost estimation. In the nitrate route case, the FCI was much higher than the one obtained for MIL-100(Fe)-S (20 M$ against 5 M$; Figure 6, top). This is a result of the higher volume that is needed in the equipment to achieve the same production capacity, as a consequence of the lower concentration and longer synthesis time. Hence, for the production of the same base amount (1 kton a year), the lower STY implies higher size of the most relevant pieces of equipment (reactor and filter) (Table S5). This production scale was considered to keep within the scales of similar studies previously reported in the literature.[18,22] It is of note that the size of the pieces of equipment to handle solids is not significantly higher, as can be seen by the calculated value of the dryer that only increased from 58 to 77 k$ (Table S5). This is due to the quantity of solid material being handled that is similar in both cases, since it is defined by the production scale considered (i.e., 1 kton).

Therefore, the difference between the two FCIs is mostly highly influenced by the reactor's dimension (for MIL-100-N, 448 m^3 and 1427 k$; for MIL-100-S, 22 m^3 and 248 k$), the optimization of this step is therefore crucial to obtain an as low as possible FCI value, as can be seen in Figure 6 (bottom). It is important to note that the total cost of the equipment, here comprising the reactor, is used to estimate the other portions

Table 3. Input and Output Per Batch to Produce 1 kton/year

MIL-100-S-5L			
	Input		**Output**
10 h synthesis			
Water (kg)	16112	MOF (kg)	1244
BTC (kg)	793	Water (kg)	126
$FeSO_4 \cdot 7H_2O$	1574		
NaOH (kg)	453	–	–
Energy (MJ/kg)	11	–	–
MIL-100-N-5L			
	Input		**Output**
62 h synthesis			
Water (kg)	347015	MOF (kg)	7711
BTC (kg)	5134	Water (kg)	779
$Fe(NO_3)_3 \cdot 9H_2O$	14807		
Energy (MJ/kg)	350	–	–

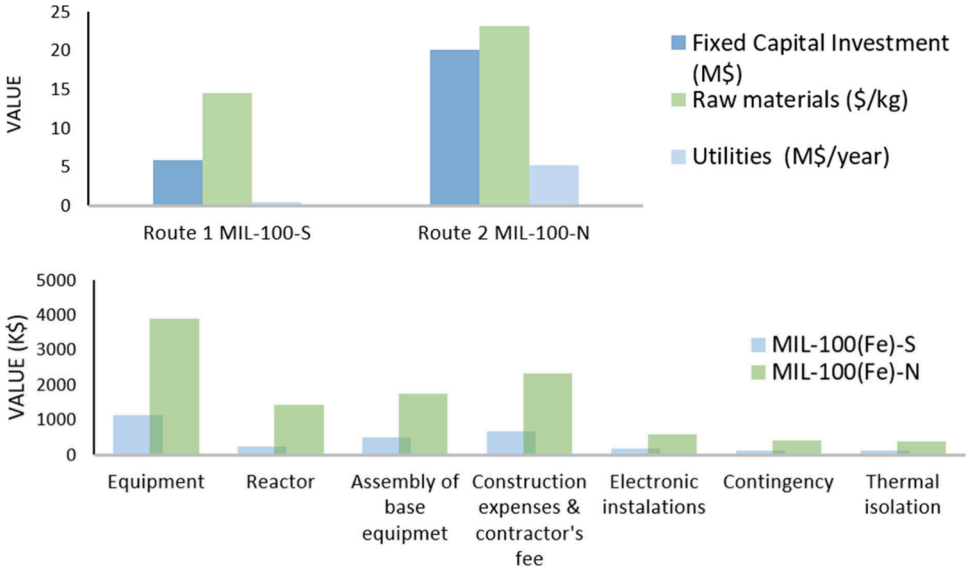

Figure 6. Impact of the main portions of the production cost for two different synthetic routes, MIL-100(Fe)-S and MIL-100(Fe)-N, and different components that influence the estimated value (the utilities considered are the electric power, the steam, and the cooling water, as depicted in Figure S11) (top). Fixed capital investment portions of the sulfate-based synthesis, compared with nitrate-based synthesis (bottom).

https://doi.org/10.1021/acs.iecr.4c02618
Ind. Eng. Chem. Res. 2025, 64, 2708−2718

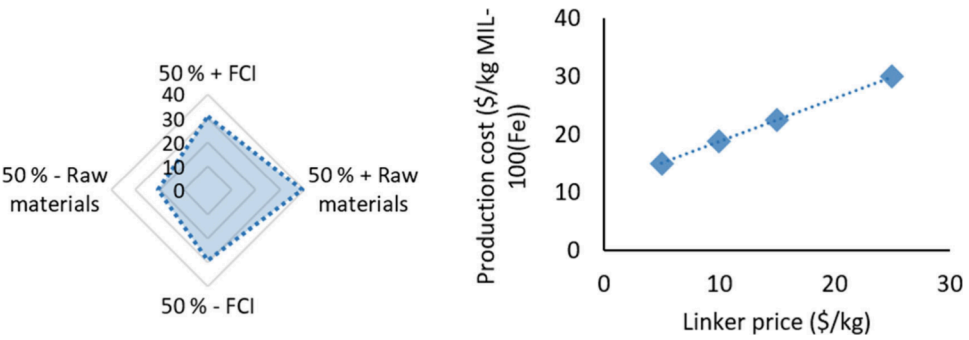

Figure 7. Sensitivity analysis of the impact of FCI and raw materials, considering more or less 50% than the base scenario, on the production cost estimated for the MIL-100-S (left) and production cost of the MIL-100-S compared with different price values for the ligand H_3BTC (right).

of the FCI, i.e., assembly of base equipment, construction expenses, contractor's fee, electric installations, contingency, and thermal isolation, by using typical chemical engineering correlations.[62] The fixed capital investment (Figure 6, bottom) then influenced several values of the cost, i.e., maintenance and repairs, plant overhead costs, operating supplies, insurance, and taxes. Other values, such as the raw materials, utilities, operating labor and supervision, rent, and depreciation, were determined based on values of the market and respective energy and mass balance.

Since the higher STY leads to lower equipment cost due to lower volume, in the sulfate-based synthesis case, the production cost is also expected to decrease. Therefore, a lower production cost of only 30 $/kg for 1 kton/year is determined for the sulfate-based synthesis when compared with the nitrate-based route, i.e., 58 $/kg. These values already include the capital costs for total investment (not only the FCI) and a project time-span of 10 years.[18] This is the first time that such a detailed comparison of production costs is reported in the literature for alternative synthesis routes that clearly indicates the critical influence of the choice of the protocols, including the starting raw materials for MOF production. Nonetheless, the nitrate-based synthesis remains the only one where high-quality nanometric rather monodisperse size particles can be obtained, which is crucial in high-end applications where the increase in cost could be justified, for instance, for biomedical or sensing applications. The production cost values obtained are also comparable to those obtained for MIL-160(Al) related to a similar process type. A low value of production cost results, therefore, from the combination of low FCI with lower operational cost, such as low raw material cost and low energy demand.

Nevertheless, it is clear that the FCI has a much lower impact contributing to the plant overhead costs maintenance and others. FCI influences, thus, less than 20% of the final value of the production cost, and even if it varies greatly, the impact on the production cost is not affected to the same extent. As we can see in Figure 7 (left), if FCI increases by 50%, the production cost increase by only 30%. Therefore, the most crucial element contributing to this low final value was the low cost considered for the raw materials (or linked elements as the yield). An increase in the raw materials cost of 50% leads to an increase in the production costs of 40% (Figure 7, left).

If the price of the linker decreases to $10/kg (the same price considered for FDCA in the production cost estimation of MIL-160(Al)), the price of MIL-100(Fe) will dramatically decrease down to $19/kg (Figure 7, right), and the trend continues with the further decrease of the linker price.

Our analysis indicates that the production cost value can be lower than 30 $/kg with the room-temperature atmospheric pressure method described in this work. This supports the use of MIL-100(Fe) for a large diversity of applications, with a value of the production cost being even similar to the first MOF considered recently for tonnage production, CALF-20.[17] In this work, it is seen by comparing the different portions that a process optimization during industrial scale-up can be targeted with a goal of an even lower production cost value. Additionally, the value of the production cost obtained and the impact of this value on the variations in FCI or raw materials, i.e., sensitive analysis, are also in line with the conclusions from MIL-160(Al) that was obtained with a similar batch synthesis method.[52]

4. CONCLUSION

The prototypical MIL-100(Fe) possesses an exceptional combination of features, i.e., high porosity, acid/redox open metal sites, green synthesis, chemical stability, and low toxicity, that caught the attention of researchers and industry. These conditions associated with higher STY of 10 $kg{\cdot}m^{-3}{\cdot}day^{-1}$, obtained after optimization of the synthesis protocol for iron nitrate as the metal source, led to a production cost of 58 $/kg while achieving a high-quality compound with rather monodisperse particle size distribution. Another optimized synthesis protocol using less corrosive iron(II) sulfate was also considered, and a higher STY, of almost 120 $kg{\cdot}m^{-3}{\cdot}day^{-1}$, was obtained. In this case, we predict that despite the common misconception that MOFs are rather expensive materials, MIL-100(Fe) appears to be a prominent MOF candidate to be produced at industrial scale with a production cost of less than 30 $/kg, as a result of the newly optimized ambient pressure green synthesis. The optimization of the synthesis protocols in this work considered all the main constraints in the industrial production, from green conditions, lack of corrosive raw materials, an easy washing method, and the use of highly concentrated solutions in order to have smaller equipment and consequently lower FCI. In addition, our new protocol does not require any increase in pressure or temperature, requiring less energy and simple pieces of industrial equipment. Nevertheless, the process design here followed a simplistic approach. Several considerations should be analyzed more deeply in the future, such as the recirculation of unreacted raw materials, which could potentially improve the production cost, or the mandatory effluent treatments which can be more crucial in the case of the nitrate-based synthesis. In summary,

https://doi.org/10.1021/acs.iecr.4c02618
Ind. Eng. Chem. Res. 2025, 64, 2708−2718

this study not only showed the potential of MIL-100(Fe) for industrial production but also allowed insight into the most important parameters for its economic viability. Finally, life-cycle assessment (LCA) studies have a strong importance, in complement to techno-economic analyses (TEA), to truly assess the environmental impact of materials over all stages of their life cycles.[63] The effect on handling, transport, disposal, recycle, and reuse need to be fully investigated to estimate their industrial potential. These studies in the field of MOFs are still very scarce,[23,63,64] and due to the growing industrial interest in MOF materials, there is a need for more systematic LCA/TEA studies when dealing with MOF commercialization studies.

■ ASSOCIATED CONTENT

Supporting Information

The Supporting Information is available free of charge at https://pubs.acs.org/doi/10.1021/acs.iecr.4c02618.

Additional characterization results of the materials: transmission IR spectrum, SEM images, average particle sizes, thermogravimetry results, PXRD patterns, nitrogen adsorption isotherms, elemental analysis, acetic acid adsorption data, production process diagram for the iron nitrate and iron sulfate production routes, detailed costs of the fixed capital investment and portions of the production costs estimation (PDF)

■ AUTHOR INFORMATION

Corresponding Authors

Farid Nouar − *Institut des Matériaux Poreux de Paris, ESPCI Paris, Ecole Normale Supérieure, CNRS, PSL University, 75005 Paris, France*; Email: farid.nouar@espci.psl.eu

Moisés L. Pinto − *CERENA, Departamento de Engenharia Química, Instituto Superior Técnico, Universidade de Lisboa, 1049-001 Lisboa, Portugal*; orcid.org/0000-0003-3061-9632; Email: moises.pinto@tecnico.ulisboa.pt

Christian Serre − *Institut des Matériaux Poreux de Paris, ESPCI Paris, Ecole Normale Supérieure, CNRS, PSL University, 75005 Paris, France*; orcid.org/0000-0003-3040-2564; Email: christian.serre@espci.psl.eu

Authors

Maria Inês Severino − *CERENA, Departamento de Engenharia Química, Instituto Superior Técnico, Universidade de Lisboa, 1049-001 Lisboa, Portugal; Institut des Matériaux Poreux de Paris, ESPCI Paris, Ecole Normale Supérieure, CNRS, PSL University, 75005 Paris, France*

Cátia Freitas − *CERENA, Departamento de Engenharia Química, Instituto Superior Técnico, Universidade de Lisboa, 1049-001 Lisboa, Portugal*; orcid.org/0000-0003-0325-691X

Vanessa Pimenta − *Institut des Matériaux Poreux de Paris, ESPCI Paris, Ecole Normale Supérieure, CNRS, PSL University, 75005 Paris, France*

Complete contact information is available at: https://pubs.acs.org/10.1021/acs.iecr.4c02618

Notes

The authors declare no competing financial interest.

■ ACKNOWLEDGMENTS

This work has received funding from the European Union's Horizon 2020 research and innovation programme under grant agreement No. 760801 \NEMOSINE. Fundação para a Ciência e a Tecnologia (FCT-MCTES) is acknowledged for funding to the Project UIDB/04028/2020, UIDP/04028/2020 (CERENA).

■ REFERENCES

(1) Hoskins, B. F.; Robson, R. Infinite Polymeric Frameworks Consisting of Three Dimensionally Linked Rod-like Segments. *J. Am. Chem. Soc.* **1989**, *111* (15), 5962−5964.

(2) Bharadwaj, P. K.; Feng, P.; Kaskel, S.; Xu, Q. Metal-Organic Frameworks and Their Applications. *Chemistry An Asian Journal* **2019**, *14* (20), 3450−3451.

(3) Byrne, F. P.; Jin, S.; Paggiola, G.; Petchey, T. H. M.; Clark, J. H.; Farmer, T. J.; Hunt, A. J.; Robert McElroy, C.; Sherwood, J. Tools and Techniques for Solvent Selection: Green Solvent Selection Guides. *Sustain Chem. Process* **2016**, *4* (1), 7.

(4) Prat, D.; Wells, A.; Hayler, J.; Sneddon, H.; McElroy, C. R.; Abou-Shehada, S.; Dunn, P. J. CHEM21 Selection Guide of Classical- and Less Classical-Solvents. *Green Chem.* **2016**, *18* (1), 288−296.

(5) Prat, D.; Pardigon, O.; Flemming, H.-W.; Letestu, S.; Ducandas, V.; Isnard, P.; Guntrum, E.; Senac, T.; Ruisseau, S.; Cruciani, P.; Hosek, P. Sanofi's Solvent Selection Guide: A Step Toward More Sustainable Processes. *Org. Process Res. Dev.* **2013**, *17* (12), 1517−1525.

(6) EHS Tool, https://emeritus.setg.ethz.ch/research/downloads/software---tools/ehs-tool.html, (Accessed June 5, 2024).

(7) Del Angel, R.; Mouchaham, G.; Nouar, F.; Tissot, A.; Serre, C. Robust and Environmentally Friendly MOFs. In *Metal-Organic Frameworks in Biomedical and Environmental Field*; Horcajada Cortés, P., Rojas Macías, S., Eds.; Springer International Publishing: Cham, 2021; pp 1−31. DOI: 10.1007/978-3-030-63380-6_1.

(8) Zhang, J.; White, G. B.; Ryan, M. D.; Hunt, A. J.; Katz, M. J. Dihydrolevoglucosenone (Cyrene) As a Green Alternative to N,N-Dimethylformamide (DMF) in MOF Synthesis. *ACS Sustainable Chem. Eng.* **2016**, *4* (12), 7186−7192.

(9) Seo, Y.-K.; et al. Large Scale Fluorine-Free Synthesis of Hierarchically Porous Iron(III) Trimesate MIL-100(Fe) with a Zeolite MTN Topology. *Microporous Mesoporous Mater.* **2012**, *157*, 137−145.

(10) Benoit, V.; Pillai, R. S.; Orsi, A.; Normand, P.; Jobic, H.; Nouar, F.; Billemont, P.; Bloch, E.; Bourrelly, S.; Devic, T.; Wright, P. A.; Weireld, G. de; Serre, C.; Maurin, G.; Llewellyn, P. L. MIL-91(Ti), a Small Pore Metal-Organic Framework Which Fulfils Several Criteria: An Upscaled Green Synthesis, Excellent Water Stability, High CO2 Selectivity and Fast CO2 Transport. *J. Mater. Chem. A* **2016**, *4* (4), 1383−1389.

(11) Kong, Z.; Niu, Z.; He, L.; Chen, Q.; Zhou, L.; Cheng, Y.; Guan, Q. In Situ Analysis of the Adsorption Behaviors of CO2 on the Surface of MIL-91(Al). *New J. Chem.* **2018**, *42* (20), 16985−16991.

(12) Cadiau, A.; Lee, J. S.; Damasceno Borges, D.; Fabry, P.; Devic, T.; Wharmby, M. T.; Martineau, C.; Foucher, D.; Taulelle, F.; Jun, C.-H.; Hwang, Y. K.; Stock, N.; De Lange, M. F.; Kapteijn, F.; Gascon, J.; Maurin, G.; Chang, J.-S.; Serre, C. Metal Organic Framework: Design of Hydrophilic Metal Organic Framework Water Adsorbents for Heat Reallocation (Adv. Mater. 32/2015). *Adv. Mater.* **2015**, *27* (32), 4803−4803.

(13) Devic, T.; Horcajada, P.; Serre, C.; Salles, F.; Maurin, G.; Moulin, B.; Heurtaux, D.; Clet, G.; Vimont, A.; Grenèche, J.-M.; Ouay, B. L.; Moreau, F.; Magnier, E.; Filinchuk, Y.; Marrot, J.; Lavalley, J.-C.; Daturi, M.; Férey, G. Functionalization in Flexible Porous Solids: Effects on the Pore Opening and the Host-Guest Interactions. *J. Am. Chem. Soc.* **2010**, *132* (3), 1127−1136.

(14) Zheng, Z.; Nguyen, H. L.; Hanikel, N.; Li, K. K.-Y.; Zhou, Z.; Ma, T.; Yaghi, O. M. High-Yield, Green and Scalable Methods for Producing MOF-303 for Water Harvesting from Desert Air. *Nat. Protoc* **2023**, *18* (1), 136−156.

(15) Dai, S.; Nouar, F.; Zhang, S.; Tissot, A.; Serre, C. One-Step Room-Temperature Synthesis of Metal(IV) Carboxylate Metal—

Organic Frameworks. *Angew. Chem., Int. Ed.* **2021**, *60* (8), 4282−4288.
(16) Chevreau, H.; Permyakova, A.; Nouar, F.; Fabry, P.; Livage, C.; Ragon, F.; Garcia-Marquez, A.; Devic, T.; Steunou, N.; Serre, C.; Horcajada, P. Synthesis of the Biocompatible and Highly Stable MIL-127(Fe): From Large Scale Synthesis to Particle Size Control. *CrystEngComm* **2016**, *18* (22), 4094−4101.
(17) Lin, J.-B.; Nguyen, T. T. T.; Vaidhyanathan, R.; Burner, J.; Taylor, J. M.; Durekova, H.; Akhtar, F.; Mah, R. K.; Ghaffari-Nik, O.; Marx, S.; Fylstra, N.; Iremonger, S. S.; Dawson, K. W.; Sarkar, P.; Hovington, P.; Rajendran, A.; Woo, T. K.; Shimizu, G. K. H. A Scalable Metal-Organic Framework as a Durable Physisorbent for Carbon Dioxide Capture. *Science* **2021**, *374* (6574), 1464−1469.
(18) Severino, M. I.; Gkaniatsou, E.; Nouar, F.; Pinto, M. L.; Serre, C. MOFs Industrialization: A Complete Assessment of Production Costs. *Faraday Discuss.* **2021**, *231* (0), 326−341.
(19) Framergy - Home, Https://Www.Framergy.Com/; Nuada - Home, Https://Nuadaco2.Com/; MOFapps - Home, Http://Www.Mofapps.Com/; Promethean Particles - Home, Https://Prometheanparticles.Co.Uk/; ProfMOF - Home, Https://Profmof.Com/; Immaterial - Home, Https://Immaterial.Com/ (Accessed June 5, 2024).
(20) Nakhla, J.; Caskey, S. Metal Organic Frameworks (MOFs), Https://Www.Sigmaaldrich.Com/US/En/Technical-Documents/Technical-Article/Materials-Science-and-Engineering/Photovoltaics-and-Solar-Cells/Metal-Organic-Frameworks/ (Accessed June 5, 2024).
(21) Ryu, U.; Jee, S.; Rao, P. C.; Shin, J.; Ko, C.; Yoon, M.; Park, K. S.; Choi, K. M. Recent Advances in Process Engineering and Upcoming Applications of Metal-Organic Frameworks. *Coord. Chem. Rev.* **2021**, *426*, 213544.
(22) DeSantis, D.; Mason, J. A.; James, B. D.; Houchins, C.; Long, J. R.; Veenstra, M. Techno-Economic Analysis of Metal-Organic Frameworks for Hydrogen and Natural Gas Storage. *Energy Fuels* **2017**, *31* (2), 2024−2032.
(23) Luo, H.; Cheng, F.; Huelsenbeck, L.; Smith, N. Comparison between Conventional Solvothermal and Aqueous Solution-Based Production of UiO-66-NH2: Life Cycle Assessment, Techno-Economic Assessment, and Implications for CO2 Capture and Storage. *Journal of Environmental Chemical Engineering* **2021**, *9* (2), 105159.
(24) Munn, A. S.; Dunne, P. W.; Tang, S. V. Y.; Lester, E. H. Large-Scale Continuous Hydrothermal Production and Activation of ZIF-8. *Chem. Commun.* **2015**, *51* (64), 12811−12814.
(25) Khabzina, Y.; Dhainaut, J.; Ahlhelm, M.; Richter, H.-J.; Reinsch, H.; Stock, N.; Farrusseng, D. Synthesis and Shaping Scale-up Study of Functionalized UiO-66 MOF for Ammonia Air Purification Filters. *Ind. Eng. Chem. Res.* **2018**, *57* (24), 8200−8208.
(26) Fröhlich, D.; Holz, A.; Henninger, S.; Lenzen, D.; Reinsch, H.; Stock, N. Method for Producing Metal-Organic Frameworks. WO2017046417A1, March 23, 2017. https://patents.google.com/patent/WO2017046417A1/en (accessed 2024-06-07).
(27) Lenzen, D.; Bendix, P.; Reinsch, H.; Fröhlich, D.; Kummer, H.; Möllers, M.; Hügenell, P. P. C.; Gläser, R.; Henninger, S.; Stock, N. Scalable Green Synthesis and Full-Scale Test of the Metal-Organic Framework CAU-10-H for Use in Adsorption-Driven Chillers. *Adv. Mater.* **2018**, *30* (6), 1705869.
(28) Shimizu, G.; Vaidhyanathan, R.; Iremonger, S.; Deakin, K.; Lin, J.-B.; Dawson, K. W. Metal Organic Framework, Production and Use Thereof. WO2014138878A1, September 18, 2014. https://patents.google.com/patent/WO2014138878A1/fr?oq=2014138878 (accessed 2024-12-04).
(29) Hovington, P.; Ghaffari-Nik, O.; Mariac, L.; Liu, A.; Henkel, B.; Marx, S. Rapid Cycle Temperature Swing Adsorption Process Using Solid Structured Sorbent for CO2 Capture from Cement Flue Gas. Social Science Research Network: Rochester, NY, March 28, 2021. DOI: 10.2139/ssrn.3814414.
(30) Horcajada, P.; Surblé, S.; Serre, C.; Hong, D.-Y.; Seo, Y.-K.; Chang, J.-S.; Grenèche, J.-M.; Margiolaki, I.; Férey, G. Synthesis and Catalytic Properties of MIL-100(Fe), an Iron(Iii) Carboxylate with Large Pores. *Chem. Commun.* **2007**, No. 27, 2820−2822.
(31) Férey, G.; Serre, C.; Mellot-Draznieks, C.; Millange, F.; Surblé, S.; Dutour, J.; Margiolaki, I. A Hybrid Solid with Giant Pores Prepared by a Combination of Targeted Chemistry, Simulation, and Powder Diffraction. *Angew. Chem., Int. Ed.* **2004**, *43* (46), 6296−6301.
(32) Campagnol, N.; Romero-Vara, R.; Deleu, W.; Stappers, L.; Binnemans, K.; De Vos, D. E.; Fransaer, J. A Hybrid Supercapacitor Based on Porous Carbon and the Metal-Organic Framework MIL-100(Fe). *ChemElectroChem.* **2014**, *1* (7), 1182−1188.
(33) Baati, T.; Njim, L.; Neffati, F.; Kerkeni, A.; Bouttemi, M.; Gref, R.; Najjar, M. F.; Zakhama, A.; Couvreur, P.; Serre, C.; Horcajada, P. In Depth Analysis of the in Vivo Toxicity of Nanoparticles of Porous Iron(III) Metal-Organic Frameworks. *Chem. Sci.* **2013**, *4* (4), 1597−1607.
(34) Quijia, C. R.; Lima, C.; Silva, C.; Alves, R. C.; Frem, R.; Chorilli, M. Application of MIL-100(Fe) in Drug Delivery and Biomedicine. *Journal of Drug Delivery Science and Technology* **2021**, *61*, 102217.
(35) Ma, X.; Lepoitevin, M.; Serre, C. Metal-Organic Frameworks towards Bio-Medical Applications. *Mater. Chem. Front.* **2021**, *5* (15), 5573−5594.
(36) Latroche, M.; Surblé, S.; Serre, C.; Mellot-Draznieks, C.; Llewellyn, P. L.; Lee, J.-H.; Chang, J.-S.; Jhung, S. H.; Férey, G. Hydrogen Storage in the Giant-Pore Metal-Organic Frameworks MIL-100 and MIL-101. *Angew. Chem., Int. Ed.* **2006**, *45* (48), 8227−8231.
(37) Wuttke, S.; Bazin, P.; Vimont, A.; Serre, C.; Seo, Y.-K.; Hwang, Y. K.; Chang, J.-S.; Férey, G.; Daturi, M. Discovering the Active Sites for C3 Separation in MIL-100(Fe) by Using Operando IR Spectroscopy. *Chem. Eur. J.* **2012**, *18* (38), 11959−11967.
(38) Yoon, J. W.; Seo, Y.-K.; Hwang, Y. K.; Chang, J.-S.; Leclerc, H.; Wuttke, S.; Bazin, P.; Vimont, A.; Daturi, M.; Bloch, E.; Llewellyn, P. L.; Serre, C.; Horcajada, P.; Grenèche, J.-M.; Rodrigues, A. E.; Férey, G. Controlled Reducibility of a Metal-Organic Framework with Coordinatively Unsaturated Sites for Preferential Gas Sorption. *Angew. Chem., Int. Ed.* **2010**, *49* (34), 5949−5952.
(39) Fu, J.-H.; Zhong, Z.; Xie, D.; Guo, Y.-J.; Kong, D.-X.; Zhao, Z.-X.; Zhao, Z.-X.; Li, M. SERS-Active MIL-100(Fe) Sensory Array for Ultrasensitive and Multiplex Detection of VOCs. *Angew. Chem., Int. Ed.* **2020**, *59* (46), 20489−20498.
(40) Giménez-Marqués, M.; Santiago-Portillo, A.; Navalón, S.; Álvaro, M.; Briois, V.; Nouar, F.; Garcia, H.; Serre, C. Exploring the Catalytic Performance of a Series of Bimetallic MIL-100(Fe, Ni) MOFs. *J. Mater. Chem. A* **2019**, *7* (35), 20285−20292.
(41) Mahmoodi, N. M.; Abdi, J.; Oveisi, M.; Asli, M. A.; Vossoughi, M. Metal-Organic Framework (MIL-100 (Fe)): Synthesis, Detailed Photocatalytic Dye Degradation Ability in Colored Textile Wastewater and Recycling. *Mater. Res. Bull.* **2018**, *100*, 357−366.
(42) Hall, J. N.; Bollini, P. Metal-Organic Framework MIL-100 Catalyzed Acetalization of Benzaldehyde with Methanol: Lewis or Brønsted Acid Catalysis? *ACS Catal.* **2020**, *10* (6), 3750−3763.
(43) Hou, P.; Zu, K.; Qin, M.; Cui, S. A Novel Metal-Organic Frameworks Based Humidity Pump for Indoor Moisture Control. *Building and Environment* **2021**, *187*, 107396.
(44) Jeremias, F.; Khutia, A.; Henninger, S. K.; Janiak, C. MIL-100(Al, Fe) as Water Adsorbents for Heat Transformation Purposes—a Promising Application. *J. Mater. Chem.* **2012**, *22* (20), 10148−10151.
(45) Severino, M. I.; Al Mohtar, A.; Vieira Soares, C.; Freitas, C.; Sadovnik, N.; Nandi, S.; Mouchaham, G.; Pimenta, V.; Nouar, F.; Daturi, M.; Maurin, G.; Pinto, M. L.; Serre, C. MOFs with Open Metal(III) Sites for the Environmental Capture of Polar Volatile Organic Compounds. *Angew. Chem. Int. Ed* **2023**, *62* (6), No. e202211583.
(46) Neves, M. I. S.; Serre, C.; Nouar, F.; Pinto, M.; Mothar, A. A.; Freitas, C. Metal Organic Frameworks for the Selective Capture of Volatil Organic Compounds Comprising Carboxylic Acid Functional

Group(s) and/or Volatile Alcohols. WO2023104665A1, June 15, 2023. https://patents.google.com/patent/WO2023104665A1/fr?oq=WO+2023%2f104665+A1 (accessed 2024-06-07).
(47) Yuan, B.; Wang, X.; Zhou, X.; Xiao, J.; Li, Z. Novel Room-Temperature Synthesis of MIL-100(Fe) and Its Excellent Adsorption Performances for Separation of Light Hydrocarbons. *Chemical Engineering Journal* **2019**, *355*, 679−686.
(48) Jeremias, F.; Henninger, S. K.; Janiak, C. Ambient Pressure Synthesis of MIL-100(Fe) MOF from Homogeneous Solution Using a Redox Pathway. *Dalton Trans.* **2016**, *45* (20), 8637−8644.
(49) Hindocha, S.; Poulston, S. Study of the Scale-up, Formulation, Ageing and Ammonia Adsorption Capacity of MIL-100(Fe), Cu-BTC and CPO-27(Ni) for Use in Respiratory Protection Filters. *Faraday Discuss.* **2017**, *201* (0), 113−125.
(50) Xu, B.; Chen, Z.; Han, B.; Li, C. Glycol Assisted Synthesis of MIL-100(Fe) Nanospheres for Photocatalytic Oxidation of Benzene to Phenol. *Catal. Commun.* **2017**, *98*, 112−115.
(51) Daturi, M.; Blasin-Aubé, V.; Yoon, J. W.; Bazin, P.; Vimont, A.; Chang, J.-S.; Hwang, Y. K.; Seo, Y.-K.; Jang, S.; Chang, H.; Wuttke, S.; Horcajada, P.; Haneda, M.; Serre, C. Room Temperature Reduction of Nitrogen Oxide on Iron Metal-Organic Frameworks. *Adv. Mater.* **2024**, *36* (31), 2403053.
(52) Panchal, M.; Nouar, F.; Serre, C.; Benzaqui, M.; Sene, S.; Steunou, N.; Marqués, M. G. Low Temperature Process for the Synthesis of Mof Carboxylate Nanoparticles. WO2018141685A1, August 9, 2018. https://patents.google.com/patent/WO2018141685A1/en?oq=US20210277042A1 (accessed 2024-06-07).
(53) Cui, S.; Qin, M.; Marandi, A.; Steggles, V.; Wang, S.; Feng, X.; Nouar, F.; Serre, C. Metal-Organic Frameworks as Advanced Moisture Sorbents for Energy-Efficient High Temperature Cooling. *Sci. Rep* **2018**, *8* (1), 15284.
(54) Ma, X.; Yu, Z.; Nouar, F.; Dovgaliuk, I.; Patriarche, G.; Sadovnik, N.; Daturi, M.; Grenèche, J.-M.; Lepoitevin, M.; Serre, C. How Defects Impact the In Vitro Behavior of Iron Carboxylate MOF Nanoparticles. *Chem. Mater.* **2024**, *36* (1), 167−182.
(55) Guesh, K.; Caiuby, C. A. D.; Mayoral, Á.; Díaz-García, M.; Díaz, I.; Sanchez-Sanchez, M. Sustainable Preparation of MIL-100(Fe) and Its Photocatalytic Behavior in the Degradation of Methyl Orange in Water. *Cryst. Growth Des.* **2017**, *17* (4), 1806−1813.
(56) Zhuang, J.-L.; Liu, X.-Y.; Mao, H.-L.; Wang, C.; Cheng, H.; Zhang, Y.; Du, X.; Zhu, S.-B.; Ren, B. Hollow Carbon Polyhedra Derived from Room Temperature Synthesized Iron-Based Metal-Organic Frameworks for Supercapacitors. *J. Power Sources* **2019**, *429*, 9−16.
(57) Tan, K. L.; Foo, K. Y. Preparation of MIL-100 via a Novel Water-Based Heatless Synthesis Technique for the Effective Remediation of Phenoxyacetic Acid-Based Pesticide. *Journal of Environmental Chemical Engineering* **2021**, *9* (1), 104923.
(58) Tian, H.; Peng, J.; Du, Q.; Hui, X.; He, H. One-Pot Sustainable Synthesis of Magnetic MIL-100(Fe) with Novel Fe3O4Morphology and Its Application in Heterogeneous Degradation. *Dalton Trans.* **2018**, *47* (10), 3417−3424.
(59) Reinsch, H.; Bueken, B.; Vermoortele, F.; Stassen, I.; Lieb, A.; Lillerud, K.-P.; Vos, D. D. Green Synthesis of Zirconium-MOFs. *CrystEngComm* **2015**, *17* (22), 4070−4074.
(60) Nivetha, R.; Gothandapani, K.; Raghavan, V.; Jacob, G.; Sellappan, R.; Bhardwaj, P.; Pitchaimuthu, S.; Kannan, A. N. M.; Jeong, S. K.; Grace, A. N. Highly Porous MIL-100(Fe) for the Hydrogen Evolution Reaction (HER) in Acidic and Basic Media. *ACS Omega* **2020**, *5* (30), 18941−18949.
(61) Steenhaut, T.; Hermans, S.; Filinchuk, Y. Green Synthesis of a Large Series of Bimetallic MIL-100(Fe,M) MOFs. *New J. Chem.* **2020**, *44* (10), 3847−3855.
(62) Peters, M. S.; Timmerhaus, K. D.; West, R. E. *Plant Design and Economics for Chemical Engineers*, 5th ed.; McGraw-Hill Chemical Engineering Series; McGraw-Hill: Boston, 2003.
(63) Grande, C. A.; Blom, R.; Spjelkavik, A.; Moreau, V.; Payet, J. Life-Cycle Assessment as a Tool for Eco-Design of Metal-Organic Frameworks (MOFs). *Sustainable Materials and Technologies* **2017**, *14*, 11−18.
(64) Hu, J.; Gu, X.; Lin, L.-C.; Bakshi, B. R. Toward Sustainable Metal-Organic Frameworks for Post-Combustion Carbon Capture by Life Cycle Assessment and Molecular Simulation. *ACS Sustainable Chem. Eng.* **2021**, *9* (36), 12132−12141.

https://doi.org/10.1021/acs.iecr.4c02618
Ind. Eng. Chem. Res. 2025, 64, 2708−2718